ISSN 2221-8688

COMPUTATIONAL BINDING STUDIES AND BIOACTIVITY EVALUATION FOR CERTAIN SCHIFF BASE METAL-COMPLEXES TRANSFORMED FROM CIPROFLOXACIN

Ahmad D. Al-Obedi*, Khansaa Sh. Al-Nama

Department of Chemistry, Collage of Science, University of Mosul, Mosul, Iraq *e-mail: ahdabd82@gmail.com

> Received 03.08.2024 Accepted 22.11.2024

Abstract: The current work focuses on using Schiff base ligand a tetra-dentate (cipro-p-phd) made from Ciprofloxacin and p-phenylenediamine. UV-visible spectroscopy, ¹H-NMR, FT-IR, TGA, (C.H.N), as well as measuring magnetic susceptibilities, fusion point and molar conductivity were used to examine the compounds. The physical measurement showed that the ligand was linked to the central atoms by oxygen atoms from carboxylate groups and nitrogen atoms from azomethine groups. Based on the measurements all compounds have tetrahedral structure, with the exception of the nickel (II) complex, which has a square planner configuration. Computer simulations and experimental data utilizing Density Functional Theory (DFT) provided additional support. Their radical scavenge activities were evaluated using the (DPPH) 2,2-Diphenyl-1-picrylhydazyl assessment in comparison to ascorbic acid. Additionally, both Gram positive and Gram negative bacteria were included in the antibacterial evaluation. The ligand was tested as a ligand with DNA gyrase employing molecular docking studies with S. aurous and E. coli.

Key words: ciprofloxacin, Schiff base, para-phenylenediamine, metal complexes, molecular docking

DOI: 10.32737/2221-8688-2025-3-449-461

Introduction

One of the classes of antibacterial agents fluoroquinolones with significant chemotherapeutic efficacy is ciprofloxacin. Fluoroguinolones have proven to be a clinically excellent treatment for bacterial infections in both hospital and community settings [1]. As of right now, antimicrobial fluoroquinolones are thought to be limited to limiting DNA synthesis and extraction by blocking DNA gyrase, in addition to topoisomerase IV and II, which are absent from the majority of human cells. In addition to limiting their use in the treatment of illnesses that these organisms cause, their low level of activity includes severe respiratory infections. However, it is most likely connected to one of the rapidly spreading resistances of quinolone. Their use has been restricted as a result. The result of this has been limitations on their use. Many of the quinolones currently available on the market or under development are only moderately effective against a broad range of Gram-positive cocci, including streptococci and staphylococci [2]. It is the only enzyme

known to be able to both unwind positive supercoils and introduce negative supercoiling into DNA. Many antibiotics target bacterial DNA gyrase, including ciprofloxacin, novobiocin, albic din, and nalidixic acid. Both direct inhibition of DNA gyrase, or "gyrase poisoning," and indirect inhibition of gyrase ATPase activity, as in the case of ciprofloxacin, are methods by which DNA gyrase inhibitors can stop bacterial growth, which stops DNA from generating negative supercoils. In order to facilitate replication, topoisomerase IV and gyrase can relax positive supertwists; Superhelical tension is released in front of the polymerase [3]. Schiff bases have a wide range of uses pharmacological, industrial, pharmaceutical, medical, and analytical fields [4-5] Since our goal is to improve the antimicrobial profile of Ciprofloxacin, many researchers have focused their attention on creating Schiff base from the drug. For these reasons, the generated tetra dentate binuclear complexes of Schiff base are the main focus of this study, which are made by the condensation reaction of para-phenyldiamine with Ciprofloxacin. The results of this research

will be useful in a variety of applications that will be covered later.

Experiments and results

Materials and Supplies.

Materials and Reagents: Every chemical used was highly pure and met the analytical reagent standard (AR). This group includes ciprofloxacin, metal chlorides, paraphenylenediamine (p-phd), and acetic glacial acid. In this experiment, dimethyl formamide (DMF) and 100% ethyl alcohol were both used

as solvents.

Formation of ligand and complexes: Drawing from our literature review [6-7] on the synthesis of the ligand and the metallic complexes, we have out Lind the preparation stages and the reagent conditions in the schematic below:

Scheme 1. Preparation process

Tools. The elements analysis was aided by the Elemental Analyzer-LCHN A10 Labtrone (C.H.N)(UK) device. Mohr analytical techniques were used to determine the contents of the Cl% in order to achieve this [8]. FT-IR spectra were captured using the Bruker IR-FT-ATR-B Spectrophotometer in the 400–4000 cm⁻¹ range. Using DMSO-d6 as the solvent, the ¹H-NMR spectra were captured on a Bio spin GmbH (400MHz) spectrometer. TG-DTG measurements were performed using the TGA-50H. The UV-3101PC Shimadzu Shimadzu was used to investigate the electronic

spectra and as solutions in DMF, the absorption spectra were captured. The calibration for the ground-up samples' magnetic susceptibilities was measured at room temperature using a Gouy balance. A Stuart spm30 melting point instrument was used to record melting points. Using a conductivity meter/Leitfahigketitsme Cond 3110 the molar conductivity of the solutions was measured at the concentration 1×10^{-3} M dissolved in DMF solvent in was determined at 28 °C.

Computational study. The (cipro-p-phd) and all complexes were optimized using

theoretical calculations using density-functional theory (DFT), which was also used to assess the complexes' electrical characteristics and thermodynamic parameters. In addition to the deployed Gaussian 09 algorithms, the 6-311++G(d,p) level of theory and the B3LYP hybrid functional were also used [9].

Applied fields. *1-Antioxidant activity assay* [10]: The free radical that is referred to 2,2-diphenyl-1-picrylhydrazyl (DPPH) was used to conduct the experiment that was intended to

assess the antioxidant activity. After first dissolving (cipro-p-phd) and its related complexes in a small quantity of DMF, they were diluted again with ethanol in this time. These substances give out hydrogen atom, which lowers the DPPH free radical and causes the color to change from deep violet to bright yellow. We evaluated the effectiveness of scavenging the DPPH radical by measuring the absorbance at 517 nm. The following equation was used to calculate the level activity of radical scavenging:

DPPH scavenging ability (%) = $\frac{Abs.control-Abs.sample}{Abs.control} \times 100$

2- Antimicrobial action [11]: The disc diffusion method was used to perform bacteriological testing. Paper discs were soaked in the ligand and its complex DMF solutions and then left to dry. Ten milliliters of dimethyl sulfoxide (DMF) were used to create solutions with concentrations of 10^{-3} M.

Paper discs were soaked after these solutions were applied. They were all dry. Following the addition of the dried paper discs to the fully formed *E. coli* and *S. aureus* culture plates, the plates were incubated for twenty-four hours at 37 °C.

3- Molecular docking studies [12]: The Auto Dock Vina 1.1.2 program was used for conducting the molecular docking simulations studies. The RCSB Protein Data Bank provided the 3D structure of DNA gyrase proteins. The two bacteria under comparison are S. aureus (PDB ID: 3g75) and E. coli (PDB ID: 1KZN). The ligand and water molecules were removed before the docking calculations for the chemical under investigation were performed. The 3D ligand geometries and conformations were created using the Chem.Axon Marvin Sketch 5.3.735 program and saved in the mol2 format. The Gaussian 09 program was used to optimize and minimize the energy of the ligand structure. Both the ligand and protein2 were prepared using Auto Dock Tools (ADT) 1.5.6. To ascertain the binding affinities, the interactions between the chemical (cipro-p-phd) and the S. aureus and E. coli DNA gyrase were mimicked. For the analysis of the ligand-targeted protein visualizer interactions, discovery studio (BIOVIA, Discovery Studio, v4.0.100.13344)

was used.

Findings and Conversation. The separated compounds' elemental analyses (Table 1) and the suggested chemical formula accord satisfactorily. The compounds' physical characteristics are presented in Table 1. The results obtained show that the metrical reaction in a stoichiometric ratio of (cipro-p-phd) 2:1 for each of those metals combined resulted in the creation of all of the distinct complexes. This approach was taken in order to achieve the complexes' creation. When building complexes, this specific process was used to successfully finish the construction. None of the complexes change color when exposed to air; they are all solid and readily soluble in DMF. Within the DMF solution, all of the complexes' molar conductance measurements were found to fall between 24 and 164 Ω^{-1} . mol⁻¹. cm², this included a remarkable variety of values [13]. The formation of a link between two chloride anions and the metal ions operating inside the inner coordination sphere is what gives the complexes their electrolytic nature. All of the complexes are classified as conductive compounds due to their high conductivity levels. In contrast, Nickel(II)-complex was categorized as a neutral compound [14]. However, as can be seen from Table 1 the geometrical shape of new complexes of Cobalt (II), Copper (II), Zinc (II) and Cadmium (II) is tetra-hedral, whereas the Nickel (II) complex has square planner. The results of both magnetic characteristics and spectral data confirm this expectation, which is consistent with what has been demonstrated in the references [15-17]. The outcomes are illustrated in Table 1.

Table 1. The crucial spectral and physical characteristics of the substances under study

Ligand and its complexe s		L= cipro-p- phd	1=[Co ₂ (L)(H ₂ O) ₂ Cl ₂]Cl ₂	2=[Ni ₂ (L)Cl ₄	3=[Cu ₂ (L)(H ₂ O) ₂ Cl ₂]Cl ₂	4=[Zn ₂ (L)(H ₂ O) ₂ Cl ₂]Cl ₂	5=[Cd ₂ (L)(H ₂ O) ₂ Cl ₂]Cl ₂	
colour		yellow	Cyan	green	Deep Walnut	Hazel	Off yellow	
Melt poi	_	282	234	195	225 243		285	
Ω^{-1} n	$10l^{-1}$	78.3	142.8	24.2	164.7	134.6	144.5	
Ca (Cl ^o Pra O	%)	/	(14.3) 13.8	(14.3) 13.5	(14.5) 13.3	(14.8) 13.7	(14.5) 13.3	
	С	(65.10) 64.68	(51.30) 50.48	(51.31) 50.72	(49.61) 48.87	(49.70) 50.92	(45.01) 44.81	
C.H .N	Н	(5.77) 4.83	(3.61) 3.52	(3.80) 3.18	(4.57) 4.48	(4.56) 3.90	(4.16) 3.92	
Cal Pra.	N	(15.22) 16.43	(12.4) 11.94	(12.4) 11.64	(11.52) 11.37	(11.52) 10.80	(10.6) 9.77	
	М	/	(.1170) 10.61	(.1170) 10.52	(2.130) 12.11	(13.32) 12.71	(19.12) 18.20	
Band UV, (cm	Vis	46727, 39692	45046,39841,37 452 16243 10891	44648,38742, 36443 22350 23538	42192 ,40652,35588 10262	46624, , 39541	46612, 39483	
Assignme nt		π→π*,n →π*	$\pi \to \pi^*, n \to \pi^*, C.$ T $^4A_2(F) \to ^4T_1(P)$ $^4A_2(F) \to ^4T_1(F)$	$\pi \rightarrow \pi^*, n \rightarrow \pi^*,$ C.T ${}^{1}A_{1}g \rightarrow {}^{1}A_{2}g$ ${}^{1}A_{1}g \rightarrow {}^{1}B_{1}g$	$\begin{array}{c} \pi {\longrightarrow} \pi^*, \\ n {\longrightarrow} \pi^*, C.T \\ {}^2T_2 {\longrightarrow}^2E \end{array} \qquad \pi {\longrightarrow} \pi^*, n {\longrightarrow} \pi^*$		$\pi{\rightarrow}\pi^*, n{\rightarrow}\pi^*$	
μ _{eff} B.M		/	3.8	0.0	1.8	Dia- magnetic	Dia- magnetic	
Th sugge struc	ested	/	Tetra-hedral	Square planner	Tetra-hedral	Tetra-hedral Tetra-hedral		

FT-IR spectroscopy. All of the infrared spectral bands that are believed to be the most crucial for all systems (Fig. 1) are listed in Table 2, as well as the assignments given to each band. Based on the statistics, the following conclusions can be made: the ligand spectra revealed a new, higher intensity band at 1626 cm⁻¹ corresponds to the imine group's frequency [18-19]. This band indicates that the amino groups have been completely absorbed by the ketogroup. Except for the Nickel(II) complex, which is made up of H2O molecules that undergo coordination and hydration processes, all complexes exhibit bands near 3472-3334 cm⁻¹ in their infrared spectra. There are multiple bands in the infrared spectrum that can be observed. The notion that these bands are in charge of the water molecules' v(O-H) vibration mode is being supported by significant elemental studies. The results of these studies indicate that these bands are in charge of the vibration mode [20]. There is a group of bands in the ligand's spectrum that can be located between 2925 and 2649 cm⁻¹. These bands are present in a variety of configurations throughout the spectrum. These bands, which represent the nitrogen vibration in the piperazine group and validate the Schiff base's zwitter ionic formula (cipro-p-phd) [21]. The stretching oscillation of the imine group v(C=N) and carboxylic $\nu(COOH)$ was found to be the cause of the two bands observed in the spectra of (cipro-p-phd). Both of these vibrations have an impact on the stretching vibration. These bands were introduced at frequencies of 1731 and 1626

cm⁻¹, respectively [22]. The Schiff basis used in this investigation was verified to be connected to the central atom by oxygen atoms of the deprotonated carboxylic group and nitrogen atoms of imine groups by overall complexes' lack of the band at 1731 cm⁻¹ and the imine group's characteristic band shifting to a lower frequency [23]. The coordination patteren of (COO⁻)group is determined by the amount of Δ (ν_{as} - ν_{s}) in our

analysis of the IR-spectrum the amount greater than 200 cm⁻¹, suggesting the connection of this group as a monodentate. Additional evidence that the bonding is improved from this angle is the appearance of additional bands of moderate strength that are observed within the range of frequencies (472-659) cm⁻¹. The assignment of these bands is caused by the stretching vibrations of both v(M-N) and v(M-O) [24].

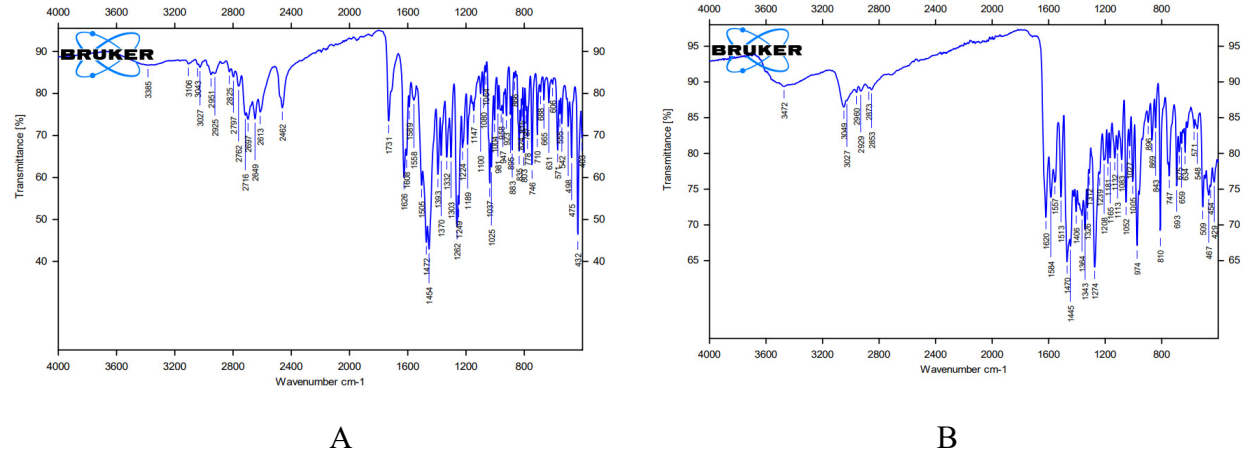


Fig. 1. The spectral output of infrared of the (cipro-p-ph) and its complexes: A-(cipro-p-ph); B-Cobalt (II) complexes

Table 2. FT-IR spectroscopy data for (cipro-p-phd) and complexes									
d and its	cipro-	[Co ₂ (cipro-p-	[Nic(cipro-	[Cu ₂ (cipro-p-	[Zn ₂ (cipro-p-	[1			

Ligand and its complexes		cipro- p-phd	[Co ₂ (cipro-p- phd) (H ₂ O) ₂ Cl ₂]Cl ₂	[Ni ₂ (cipro- p-phd)Cl ₄]	[Cu ₂ (cipro-p- phd) (H ₂ O) ₂ Cl ₂]Cl ₂	[Zn ₂ (cipro-p- phd) (H ₂ O) ₂ Cl ₂]Cl ₂	[Cd ₂ (cipro-p-phd) (H ₂ O) ₂ Cl ₂]Cl ₂
	H ₂ O; - COOH; v(OH);	3385	3472	/	3375	3478	3334
	COOH v(C=O)	1731	/	/	/	/	/
	v (C=N)	1626	1620	1620	1617	1612	1610
	v (COO-)asy	/	1513	1560	1512	1554	1531
FT-IR spectrum	v (COO-)sy	1370	1312	1335	1312	1342	1300
	v (O- M)	/	467	475	546	542	477
	v(N-M)	/	659	632	653	625	659

¹H-NMR Analysis

Fig. 2 shows ¹H-NMR spectra of the ligand and Cadmium complex combination obtained in DMSO at room temperature, using TMS as the internal standard. The Cadmium (II) complex spectrum's loss of the characteristic singlet at 15.12 ppm, which was previously identified in the ligand's spectrum, indicates that the ligand's coordination with the protonated carbonyl group's oxygen atom [25]. Additional bands may be visible in the Cadmium (II)-complex's ¹H-NMR spectra at concentrations of (4.32-4.58) ppm. These

bands are the result of coordinated water molecules existing within the complex, which is what causes them to appear. As stated, we can summarize the chemical changes δH in ppm.

A-(cipro-p-phd): 1.18-1.2 ppm, δ H(-CH₂, -CH)/cyclopropan), δH,(-CH₂ aliphatic 3.34-3.85), $\delta H(-NH; piperazine = 2.48), \delta H(-NH₂⁺=$ δ H(-COOH=15.12), 2.49), δΗ (-CH aromatic=7.50-9.41). B-[Cd₂(cipro-pphd)(H_2O)₂Cl₂]Cl₂, δH (-CH₂ and -CH =1.2- $\delta H(-NH_2^+=2.49),$ 1.35), $\delta H(-NH;$ piperazine=2.09), δ H(-CH aromatic=7.60-8.70), δ H(-CH₂ aliphatic=3.18-3.86).

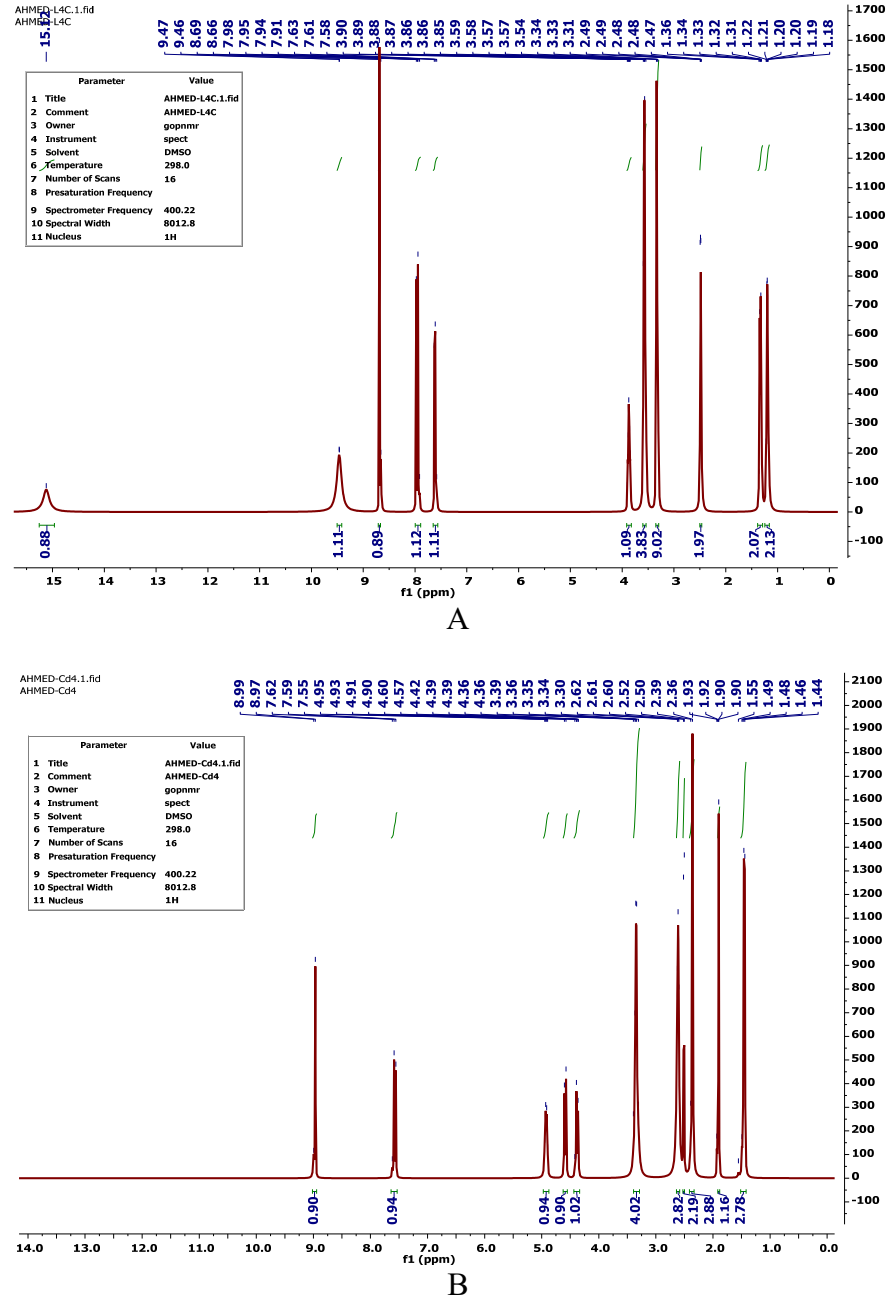


Fig. 2. The ¹H-NMR-charts: A-(cipro-p-phd), B- [Cd₂(cipro-p-phd) (H₂O)₂Cl₂]Cl₂

Thermal analysis measurements (TGA). Thermogravimetric studies (TGA) (Fig. 3) were performed on isolated solid complexes to collect information about their thermal stability, identify the type of water molecules linked to the

complexes, and suggest a generic thermolysis approach [26]. The phases of complicated breakdown were thoroughly examined and enumerated in Table 3.

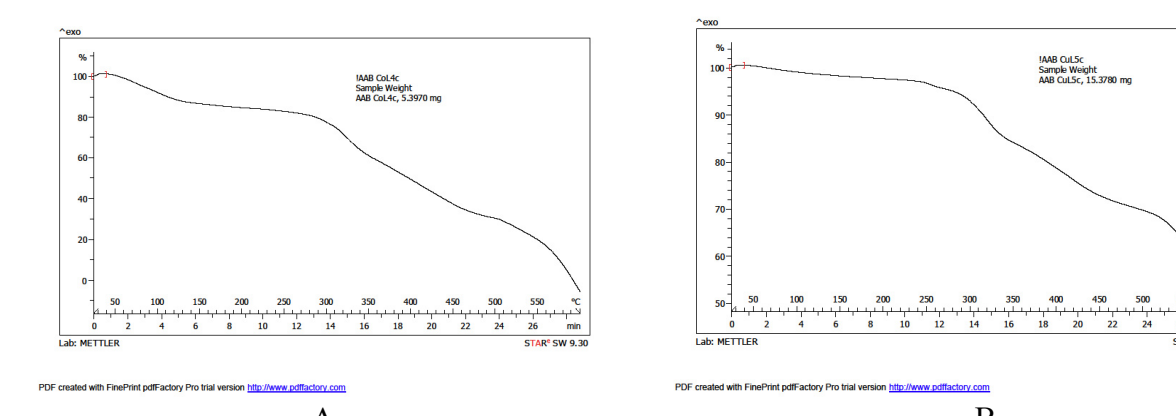


Fig. 3. Thermogravimetric analysis for A-[Co₂(cip-p-phd) (H₂O)₂Cl₂] Cl₂ and B-[Cu₂(cip-p-phd) (H₂O)₂Cl₂] Cl₂

Table 3. Thermal disintegration of the complexes

Isolated complexes	Disintegration steps	Temperature. max ∘c	Lost groups
[Co ₂ (cipro-p-phd) (H ₂ O) ₂ Cl ₂]Cl ₂ .6H ₂ O	first step, second step	25-135,	6H ₂ O (lattice), 2H ₂ O (coordinated) 2CO ₂ +3N ₂ +2HF +2HCl + 3H ₂ + 2NO
(Co ₂ C ₄₀ H ₄₈ N ₈ O ₈ F ₂ Cl ₂) Molecular Wight:1030.43 g/mol	loss Complete	320-600	+17C ₂ H ₂ 2CoO + 4C
[Ni ₂ (cipro-p-phd)Cl ₄].5H ₂ O	first step, second step	25-125,	5H ₂ O (lattice), 2HF+4NO+2HCl+2N ₂
(Ni ₂ C ₄₀ H ₄₀ N ₈ O ₈ F ₂ Cl ₂) Molecular Wight:1030.45 g/mol	loss Complete	125- 600	+18C ₂ H ₂ + 2NiO+4CO
[Cu ₂ (cipro-p-phd)(H ₂ O) ₂ Cl ₂]Cl ₂ .3H ₂ O	first step, second step	25-125,125- 290	3H ₂ O (lattice), 2H ₂ O (coordinated) 2HCl + 2HF + CO + 17C ₂ H ₂ +2NO + 3N ₂
(Cu ₂ C ₄₀ H ₄₈ N ₈ O ₆ F ₂ Cl ₂) Molecular Wight:1039.73 g/mol	loss Complete	290- 600	$Cu_2O + 5C + 3H_2$
[Zn ₂ (cipro-p- phd)(H ₂ O) ₂ Cl ₂]Cl ₂ .6H ₂ O	first step, second step	25-125,125- 355	6H ₂ O /lattice, 2H ₂ O/ coordinated C ₂ N ₂ + 2HF + 2HCl 18C ₂ H ₂ + 2H ₂
(Zn ₂ C ₄₀ H ₄₈ N ₈ O ₁₃ F ₂ Cl ₄) Molecular Wight:1043.42 g/mol	loss Complete	355- 600	+5N ₂ 4C +2ZnO
[Cd ₂ (cipro-p-	first step, second step	25-125, 125- 300	6H ₂ O/ lattice, 2H ₂ O/ coordinated 18C ₂ H ₂ + C ₂ N ₂ + 2HF + 2HCl + 2H ₂
phd)(H ₂ O) ₂ Cl ₂]Cl ₂ .6H ₂ O (Cd ₂ C ₄₀ H ₄₈ N ₈ O ₁₃ F ₂ Cl ₂) Molecular Wight:1137.47 g/mol	loss Complete	300- 600	+5N ₂ 2CdO + 4C

The following formulas (Table 3) for the ligand and complexes can be suggested based on the measurement above.

Bacteriological Testing. When compared to ciprofloxacin, the findings of the antibacterial activity research showed that every metal

complex was efficient against the tested microorganisms (Fig. 4). One possible explanation for the potent antibacterial action of (cip-p-phd) is to claim that only lipid-soluble substances can get through the lipid membrane that envelops the cell. This is among the most

likely reasons. Lipo solubility is a crucial characteristic that is involved in determining the antibacterial activity of drugs that belong to this category. From this moment on, the ligand's polarity will be reduced more than it was before.

It will be like this. This is because donor groups will start to overlap with the ligand orbital. Furthermore, it enhances the ligand's lipophilicity and promotes the π -electrons' dispersion throughout (cipro-p-phd) ring [27].

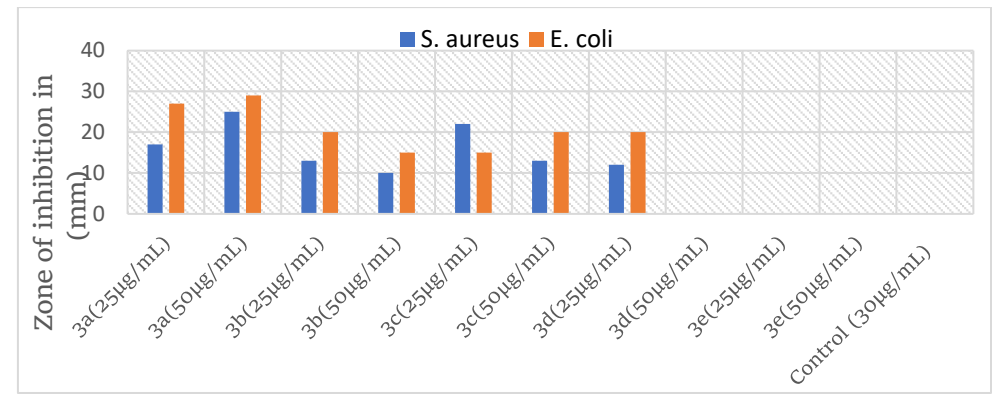


Fig. 4. Data from antimicrobial screening of (cipro-p-phd) and the complexes

Molecular Docking Analysis. According to the outcomes of molecular docking, the chemical (cipro-p-phd) exhibits binding modes with DNA gyrase that are very similar to the binding mode of clorobiocin. The development of (cipro-p-phd)-protein complex in the *E. coli* DNA gyrase active site is depicted in Fig. 5, (1i-1j) (ID: 1KZN), with a ΔG value of the linkage energy of -7.8 kcal/mol. Green dotted lines demonstrate the three amino acids' hydrogen

bonding GLN 72, LYS57, THR167 stabilized the complex that was created. Different colored dotted lines are used to indicate various bonding contact types, such as Halogen-Fluorine, pi-Anion, pi-Sigma and pi-alkyl, among others. The ligand-protein combination within the $E.\ coli$ DNA gyrase active site exhibits a ΔG value of the binding energy of -5.9 k calorie/mol when compared to the well-known antibiotic Ciprofloxacin [28] (2i-2j).

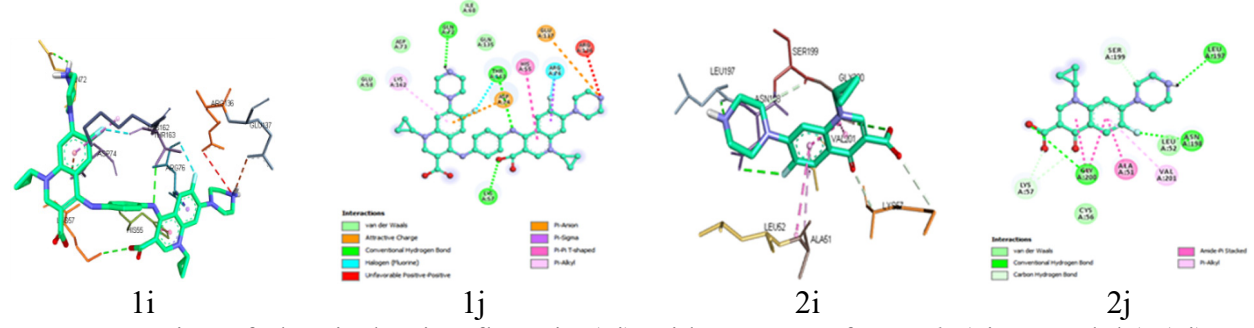


Fig. 5. Interaction of chemical: Ciprofloxacin (2i) with enzyme of *E. coli* (cipro-p-phdn) (1i) and (1KZN: ID) in a 3Dimention ribbon. Compound (cipro-p-phdn) (1j) and Ciprofloxacin (2j) show 2Dimention interactions with specific amino acid residues of *E. coli* (1KZN: ID) enzyme.

However, Fig. 6 (3f-3g) demonstrated the development of a compound (cipro-p-phd)-protein complex with a ΔG the binding energy's value -8.6 k calorie/mol in the active site of *S. aureus* DNA gyrase (ID: 3g75). Three amino acid hydrogen bonds stabilized the ligand-protein combination, LYS 78, THR 212, GLN 66. Along many bonding contact kinds (such as: pi-Sigma 80, pi-alkyl with VLA: 174, salt bridge

224 GLU), Different kinds of bonding interactions and hydrophobic interactions (like van der Waal's, pi-cation and pi-Alkyl etc.). In contrast to the well-known antibiotic ciprofloxacin, (cipro-p-phd) -protein combination within the ΔG binding energy of the *S. aureus* DNA gyrase's active site is -5.5 k calorie /mol (4f-4g).

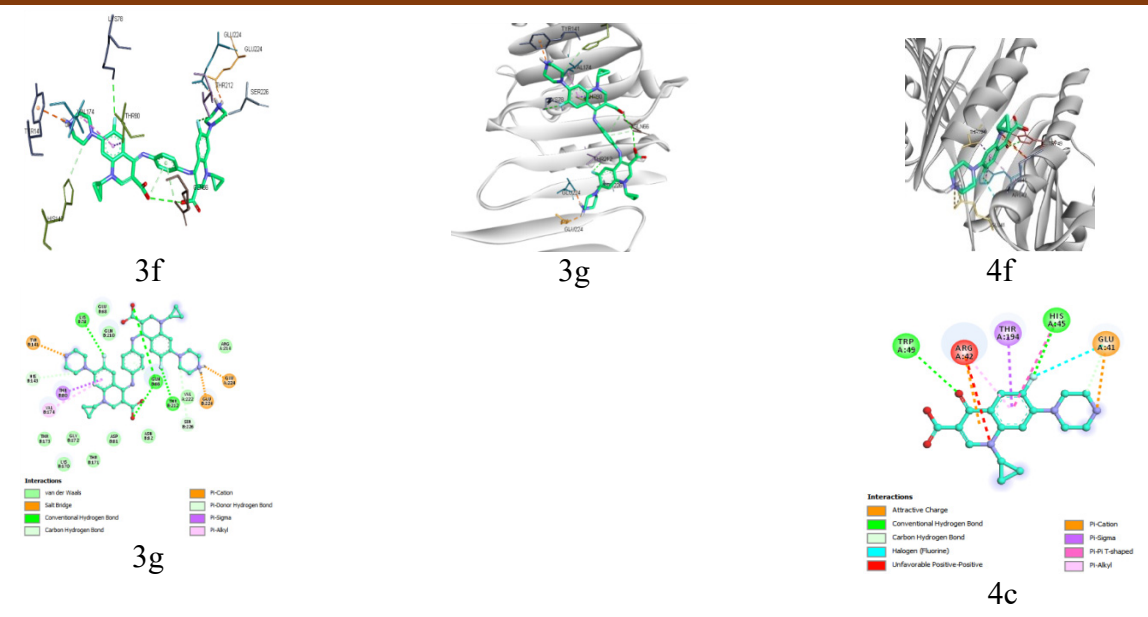


Fig. 6. Interaction of chemical: (cipro-p-phd) (3f), A stick model for Ciprofloxacin (4i) and (cipro-p-phd) (3i), Ciprofloxacin (4f) and enzyme of *S. aureus* (ID: 3g77) in a 3Dimention ribbon exhibit three dimension interactions with specific amino acid residues of the *S. aureus* (ID: 3g76) enzyme. Ciprofloxacin (4c) Compound with (cipro-p-phd) (3c) demonstrate two-dimensional interactions with specific amino acid residues of S. aureus (ID: 3g77) enzymes.

Activity of antioxidant measurement. The presence of NH-groups may be the cause of the Schiff base ligand's and its copper complex's high Radical Scavenging Activity (RSA). These groups are capable of giving DPPH an electron or a hydrogen atom, which creates a stable free radical. The high RSA is a result of these. This

radical can be stabilized via the delocalization process. They can also operate as scavengers of free radicals, as demonstrated by their ability to transfer electrons and/or hydrogen atoms. However, none of the compounds exhibited better radical scavenging efficacy than the standard ascorbic acid Table 4.

Table 4. That oxidation measurements of the compounds							
Complex	The percentage of ligand and its compounds that scavenge						
Compress	20 ppm	40 ppm	60 ppm				
(cipro-p-phd)	72.8	70.8	70.9				
[Co ₂ (cipro-p-phd) (H ₂ O) ₂ Cl ₂]Cl ₂	71.2	70.7	68.2				
[Ni2(cipro-p-phd) Cl4]	76.6	72.3	72.5				
[Cu ₂ (cipro-p-phd)(H ₂ O) ₂ Cl ₂] Cl ₂	73.3	75.9	79.5				
Ascorbic acid(Vit.C)	84	86	92				

Table 4. Anti-oxidation measurements of the compounds

Active antioxidant properties are present in both the ligand and the copper complex it forms. The measurements were used to determine the percentage of scavenging that indicated the activity of (cipro-p-phd) and its Copper (II) complex. 20 ppm, 40 ppm, and 60 ppm of [Cu₂(cipro-p-phd)(H₂O)₂Cl₂]Cl₂ 73.3, 75.9, and 79.5 respectively. Ascorbic acid is represented

numerically by the numerals 86, 92, and 84 (A.A). Strong free radical scavenging activity was demonstrated by the Schiff base ligand and its copper complex against the generation of free radicals brought on by (2,2-diphenyl-1-picrylhydrazyl) at a variety of concentrations. This was demonstrated by conducting a number of tests to illustrate the concept. The three

different concentrations available are 20 μ g/ml, 40 μ g/ml, and 60 μ g/ml. The available options are made up of these values. Actual ascorbic acid is now the standard used for ascorbic acid measurement [29].

Computational studies (DFT). We can determine the specifics of the highest occupied and lowest unoccupied molecular orbital energies (HOMO and LUMO) by: application of Frontier Molecular Orbital (FMO), as illustrated

in Fig. 7. Understanding everything pertaining to the electrical arrangement and reactivity of different kinds of molecules requires an understanding of these ideas. The LUMO and HOMO energies have been computed using Density Function Theory $\frac{B3LY}{P6-311++G(d,p)}$ system, Several parameters that are stated in Table 5 and computed using the following equations are obtained through this system [30]:

- 1. The energy of Ionization = $-E_{HOMO}$
- 2. The Gap energy (ΔE_{GAP}) = (E_{LUMO} E_{HOMO})
- 3. The Hardness of Global (η) = (E_{LUMO}- E_{HOMO}/2)
- 4. The Electronegativity of Absolute $(\gamma) = (1+A/2)$
- 5. The Index of Electrophilicity (ω) = ($\chi^2 / 2 \eta$)
- 6. The Softness Chemical $(\sigma) \rightarrow (\sigma = 1/\eta)$

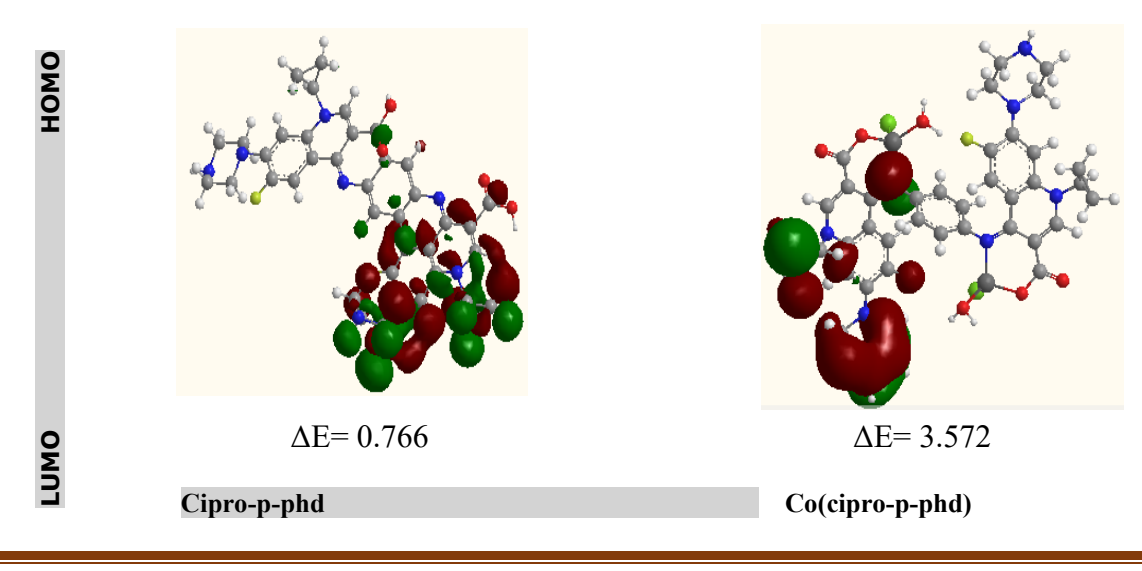
The LUMO and HOMO energy gap can be used to identify a variety of molecular characteristics, including optical polarizability, kinetics, chemical stability, and chemical hardness/softness [31]. When compared to hard molecules, a molecule with a smaller energy gap is more effective since it is a soft molecule with a high degree of polarization. Among the other

complexes in our study, the Nickel (II)-complex has the previously mentioned features. The stability sequence of the molecule can be summed up as follows using the DFT data: Zinc(II)

complex>Cadmium(II)complex>Copper(II)complex>Cobalt(II)complex>(cipro-p-phd)>Nickel(II) complex.

Table 5. Quantum chemical characteristics calculated for cipro-p-phd and its complexes

Ligand and Complexes	ЕНОМО	<i>E</i> LUMO	ΔE	I	A	ΔN	η	σ	χ
L(cipro-p-phd)	-4.553	-2.078	2.472	4.553	2.078	1.238	3.317	0.808	1.492
L(Co)	-2.878	-2.118	3.115	10.728	7.615	1.557	9.172	0.643	-0.693
L(Ni)	-2.877	-2.115	0.766	2.878	2.115	0.383	2.498	2.617	5.892
L(Cu)	-5.141	-1.571	3.571	5.141	1.571	1.786	3.356	0.562	1.023
L(Zn)	-5.988	-0.921	5.068	5.988	0.921	2.536	3.455	0.394	0.699
L(Cd)	-5.217	-0.869	4.347	5.217	0.869	2.175	3.043	0.461	0.912



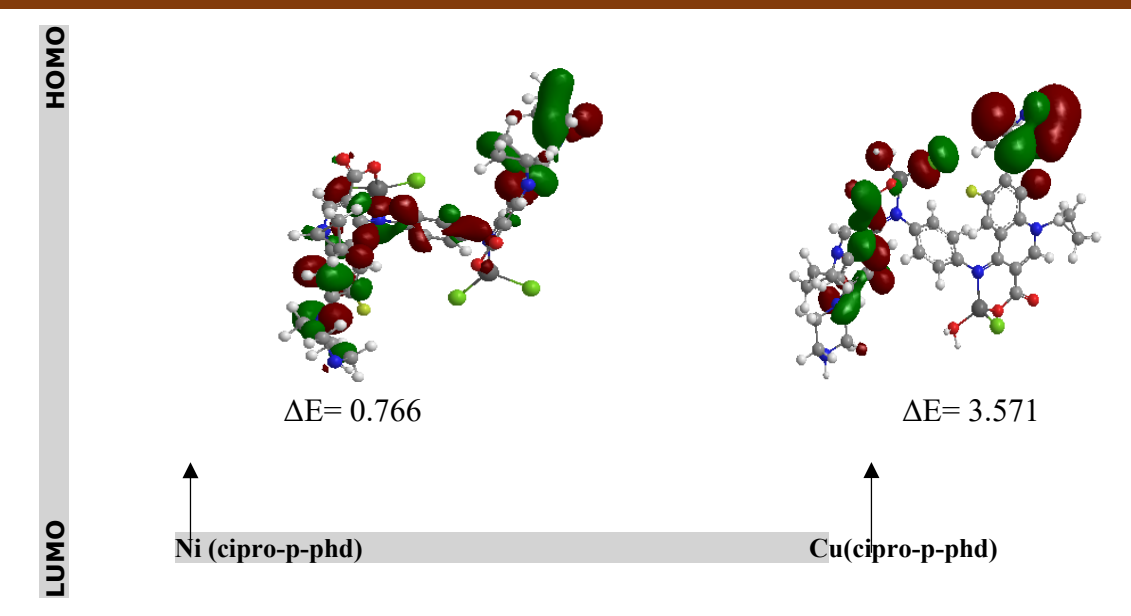


Fig. 7. Optimized structures and HOMO / LUMO of the cipro-p-phd and its complexes

Conclusion

We can describe the key finding by using the obtained results. Tetra dentate bi-negative charge behavior is displayed by the ligand. With the exception of the Nickel (II)complex, which has a square shape, all complexes have a tetrahedral structure. The ligand and its complexes exhibit antioxidant properties by occupying free radicals, such as ascorbic acid.

The ligand shows high efficacy against certain bacterial species. Moreover, a molecular docking investigation that demonstrated the compound's ability to connect with bacterial DNA gyrase has validated these findings. Comparing the chosen compound's binding energy to that of the antibiotic Ciprofloxacin, it can be said that it has the potential to be an antibacterial agent.

Acknowledgment. This research has been finished with the ongoing assistance of every employee in the labs and research facilities at the University of Mosul and the College of Science. We sincerely thank everyone of them.

References

- 1. Elshafie H.S., Sadeek S.A., Camele I., Mohamed A.A. Biochemical characterization of new gemifloxacin schiff base (GMFX-ophdn) metal complexes and evaluation of their antimicrobial activity against some phyto-or human pathogens. *International Journal of Molecular Sciences*. 2022, **Vol. 23(4)**, p. 2110. DOI: 10.3390/ijms23042110
- Sadeek S.A., EL-Shwiniy W.H., Zordok W.A., EL-Didamony A.M. Spectroscopic, structure and antimicrobial activity of new Y(III) and Zr(IV) ciprofloxacin. Spectrochim. 2011, Vol. 78, p. 854–867. DOI: 10.1016/j.saa.2010.12.048
- 3. Tirmazi S.A., Qadir M.A., Ahmed M., Imran M., Hussain R., Sharif M., Yousaf M., Muddassar M. Levofloxacin and sulfa drugs

- linked via Schiff bases: Exploring their urease inhibition, enzyme kinetics and in silico studies. *Journal of Molecular Structure*. 2021, **Vol. 1235**, 130226. DOI: 10.1016/j.molstruc.2021.130226
- 4. Abdalrazaq E., Jbarah A.A., Al-Noor T.H., Shinain G.T., Jawad M.M. Synthesis, DFT calculations, DNA interaction, and antimicrobial studies of some mixed ligand complexes of oxalic acid and Schiff base trimethoprim with various metal ions. *Indonesian Journal of Chemistry*. 2022, Vol. 22(5), p. 1348-1364. DOI: 10.22146/ijc.74020
- 5. Patil M.K., Masand V.H., Maldhure A.K. Schiff base metal complexes precursor for metal oxide nanomaterials: a review. *Curr*

- *Nanosci.* 2021, **Vol. 17(4)**, p. 634-45. DOI: 10.2174/1573413716999201127112204
- Mahmood Z.M., Saied Sh.M., Saleh M.Y. Deep eutectic solvent (reline) as catalytic system in synthesis of schiff bases derived from glucose and different amines. *Chemical Problems*, 2024, Vol. 22(3), p. 281-289. DOI: 10.32737/2221-8688-2024-3-281-289
- 7. Mammadova S.M., Seyidova Ch.M., Guliyeva C.E., Racabli A.R., Aslanova H.F., Shikhverdiyeva N.T., Rahimli N.T., Zeynalov N.A. Obtaining a hydrogel based on chitosan, study its structure and sorbtion ability with levofloxacin antibiotics. *Chemical Problems*, 2021, **Vol. 19(4)**, p. 215-223. DOI: 10.32737/2221-8688-2021-4-215-223
- 8. Baran N.Y., Saçak M. Preparation of highly thermally stable and conductive Schiff base polymer: Molecular weight monitoring and investigation of antimicrobial properties. *Journal of Molecular Structure*, 2018, **Vol. 1163**, p. 22-32. DOI: 10.1016/j.molstruc.2018.02.088
- 9. Szabo, A., Nostlund N. *Modern Quantum Chemistry*. 1st Ed. Dover Publication: New York. 1989. 461p.
- Nauman Ali N., Ahmad Sh., AbdEl-Salam N.M., Ullah R., Nawaz R., Ahmad S. Synthesis and evaluation of antioxidant and antimicrobial activities of Schiff base Tin (II) complexes. *Trop. J. Pharm. Res.*, 2016, Vol. 15, p. 2693-2700. DOI: 10.4314/tjpr.v15i12.22
- 11. Kavitha N., Lakshmi P.V.A. Synthesis, characterization and Thermogravimetric analysis of Co(II),Ni(II),Cu(II) and Zn(II) complexes supported by ONNO tetra dentate Schiff base ligand derived from hydrazine benzoxazine. *Journal of Saudi a Chemical Society*, 2017, **Vol. 21**, p. 5457-5466. DOI: 10.1016/j.jscs.2015.01.003
- 12. Nicholls D. The chemistry of iron, cobalt and nickel: comprehensive inorganic chemistry, Elsevier. Vol. 24. 2013.
- 13. Elshafie H., Sadeek S., Zordok W., Mohamed A. Meloxicam and Study of Their Antimicrobial Effects against Phyto- and Human Pathogens. *Molecules*, 2021, **Vol. 26(5)**, p. 1480. DOI: 10.3390/molecules26051480
- 14. Sadeek S.A., El-Attar M.S., El-Hamid S.M.A. Synthesis and characterization and

- antibacterial activity of some new transition metal complexes with ciprofloxacin-imine. *Bull. Chem. Soc. Ethiop.* 2015, **Vol. 29**, p. 259–274. DOI: http://dx.doi.org/10.4314/bcse.v29i2.9
- 15. Ali A.M., Al-Noor T.H., Abdalrazaq E., Jbarah A.A.Q., Synthesis and DFT study of the complexation of Schiff Base derived curcumin and L-tyrosine with Al (III), Ag (I), and Pb (II) metal ions. *Indonesian Journal of chemistry*, 2021, **Vol. 21(3)**, p. 708-724. DOI: 10.22146/ijc.62188
- 16. Elshwiniy W.H., Ibrahim A.G., Sadeek S.A., Zordok W.A. Ligational, density functional theory, and biological studies on some new Schiff base 2-(2-hydroxyphenylimine) benzoic acid (L) metal complexes. *Appl. Organomet. Chem.* 2020, **Vol. 34**, p. 5819. DOI: 10.1002/aoc.5819
- Lemoui R., Allal H., Hannachi D., Djedouani A., Ramli I., Habila I., Zabat M., Merazig H., Stoeckli-Evans H., Ghichi N. Synthesis, Crystal structure, Hirshfeld surface interactions, anti-corrosion analysis, DFT calculations, Docking studies and evaluation of the antioxidant activity of a new zwitterion Schiff base. *Journal of Molecular Structure*, 2023, Vol. 1286, p. 135569. DOI: 10.1016/j.molstruc.2023.135569
- 18. Al-qasii N.A.R., Bader A.T., Mosaa Z. Synthesis and characterization of a novel azo-dye Schiff base and its metal ion complexes based on 1,2,4-triazole derivatives. *Indones. J. Chem.* 2023, **Vol.** 23(6), p. 1555–1566. DOI: 10.22146/ijc.83509
- 19. Sadeek S.A., EL-Shwiniy W.H., Zordok W.A., EL-Didamony A.M. Spectroscopic, structure and antimicrobial activity of new Y(III) and Zr(IV) ciprofloxacin. Spectrochima Acta. Part A, 2011, Vol. 78, p. 854-867. DOI: 10.1016/j.saa.2010.12.048
- Sultana N., Arayne M.S., Rizvi S.B.S., Haroon U., Mesaik M.A. Synthesis, spectroscopic and biological evaluation of some levofloxacin metal complexes. *Medicinal Chem. Res.* 2013, Vol. 22(3), p. 1371-1377. DOI: 10.1007/s00044-012-0132-9
- 21. Hendradi E., Hariyadi D.M., Adrianto M.F. The effect of two different crosslinkers on in

- vitro characteristics of ciprofloxacin-loaded chitosan implants. *Research in Pharmaceutical Sciences*, 2018, **Vol. 13(1)**, p. 38-46. DOI: 10.4103/1735-5362.220966
- 22. Hassan B.A., Hamed F.M. Synthesis and pharmaceutical activity of triazole Schiff bases with theoretical characterization. *Chemical Problems*, 2024, Vol. 22(3), p. 332-341. DOI: 10.32737/2221-8688-2024-3-332-341
- 23. Sami S., Shaalan N. Synthesis, Structure and Biological Activity Studies of New Metal Ion Complexes Based on 3-[(3-Hydroxynaphthalene-2-yl-ethylidene)-hydrazono]-1, 3-dihydro-indol-2-one. *Indonesian Journal of Chemistry*, 2024, Vol. 24(2), p. 370-378. DOI: 10.22146/ijc.87359
- 24. Shi W.K., Deng R.C., Wang P.F., Yue Q.Q., Liu Q., Ding K.L., Yang M.H., Zhang H.Y., Gong S.H., Deng M., Liu W.R. 3-Arylpropionylhydroxamic acid derivatives as Helicobacter pylori urease inhibitors: Synthesis, molecular docking and biological evaluation. *Bioorganic & medicinal chemistry*, 2016, Vol. 24(19), p. 4519-4527. DOI: 10.1016/j.bmc.2016.07.052
- 25. Putaya H.A.N., Ndahi N.P., Bello H.S., Mala G., Osunlaja A.A., Garba H. Synthesis, characterization and antimicrobial analysis of Schiff bases of o-phenylenediamine and 2-aminopyridine-3-carboxylic acid with ofloxacin and their metal (II) complexes. *Int. J. Biol. Chem. Sci.* 2020, **Vol. 14(1)**, p. 263-278. DOI:10.4314/ijbcs.v14i1.22
- 26. Fatullayeva P.A. Synthesis, structure and properties of complexes Cu(II) Co(II), Ni(II), Vo(II) with (3,5-ditretbutyl-2-hydroxybenzyl)-2-hydroxybenzoyl-

- hydrazide. *Chemical Problems*, 2018, **Vol. 16(4)**, p. 519-523. DOI: 10.32737/2221-8688-2018-4-519-523
- 27. Khan M., Ali M., Juyal D. Ciprofloxacin metal complexes and their biological activities: A review. *The Pharma Innovation Journal*, 2017, **Vol. 6(5)**, p. 73-78.
- 28. Norouzbahari M., Salarinejad S., Güran M., Şanlıtürk G., Emamgholipour Z., Bijanzadeh H.R., Toolabi M., Foroumadi A. Design, synthesis, molecular docking study, and antibacterial evaluation of some new fluoroquinolone analogues bearing a quinazolinone moiety. *Daru Journal of Pharmaceutical Sciences*, 2020, **Vol. 28(2)**, p. 661-672. DOI: 10.1007/s40199-020-00373-6
- 29. Abdul-Rida N.A., Talib K.M. New chalcone derivatives as anticancer and antioxidant agents: synthesis, molecular docking study and biological evaluation. *Chemical Problems*, 2024, **Vol. 22(2)**, p. 177-186. DOI:10.32737/2221-8688-2024-2-177-186
- 30. Dubeym A., Dotolo S., Ramteke P.W., Facchiano A., Marabotti A. Searching for chemise inhibitors among chamomile compounds using a computational-based approach. *Biomolecules*, 2018, Vol. 9(5), p. 1-15. DOI: 10.3390/biom9010005
- 31. Rauf A., Shah A., Munawar Kh.Sh., Khan A.A., Abbasi R., Yameen M.A., Khan A.M., Khan A.R., Qureshi I.Z., Kraatz H.-B., Ziaur-Rehman. Synthesis, spectroscopic characterization, DFT optimization and biological activities of Schiff bases and their metal (II) complexes. *Journal of Molecular Structure*, 2017, Vol. 1145, p. 132-140. DOI: 10.1016/j.molstruc.2017.05.098